

Analysis of the energy distribution of escaping suprathermal ions in neutral-beam injection phase of the TJ-II stellarator

M. Martínez¹, B. Zurro², A. Baciero², D. Jiménez-Rey², V. Tribaldos³

¹*Universidad Carlos III de Madrid, Leganés, Spain.*

²*Laboratorio Nacional de Fusión, CIEMAT, Av. Complutense 40, 28040 Madrid, Spain.*

³*Departamento de Física, Universidad Carlos III de Madrid, Leganés, Spain*

E-mail contact of main author: *marcos.martinez@externos.ciemat.es*

INTRODUCTION. Detailed knowledge of loss mechanisms of fast or suprathermal ions associated to fusion processes or heating methods is of paramount interest in plasma fusion research. In this work, the ion distribution function on suprathermal ions escaping from TJ-II plasmas during the neutral beam injection (NBI) phase of the plasma is being investigated to extend those already reported studies mainly for electron cyclotron resonance heating (ECRH) plasmas [1,2]. These ions are monitored with a flexible luminescent probe (LP) [3], which is operating in a pulse energy discrimination mode [4] and it is located at the edge of the TJ-II stellarator. This work is focused on studying the behaviour of suprathermal ions energy distributions under two different conditions: when the NBI heating starts after an ECRH and when initiating the plasma solely with NBI heating. Also the pellet injection on the second type of discharge (solely with NBI heating), and its effects on suprathermal ions energy distribution are studied. We will discuss its empirical behaviour.

EXPERIMENTAL. TJ-II is a four-period, low magnetic shear stellarator with major and averaged minor radii of 1.5 m and ≤ 0.22 m, respectively. Central electron densities and temperatures up to $1.7 \times 10^{19} \text{ m}^{-3}$ and 1 keV respectively are achieved for plasmas created and maintained by ECRH at the second harmonic ($f = 53.2 \text{ GHz}$, $P_{ECRH} \leq 500 \text{ kW}$) [5]. The magnetic confinement of TJ-II plasmas involves four main magnetic field components, two of them (CC and HX) produced by the central coil system [6]. The steady-state values of the CC and HX currents are 10 kA and 4.8 kA, respectively. The associated toroidal electric fields induced are 2.8 and 1 V/turn, respectively, corresponding to a total induced toroidal field of 0.35 V/m, at the lower limit of those used for ohmic break-down in tokamaks [7]. NBI launch times are between 960 and 980 ms, and it is produced for up to 120 ms while CC and HX are on the plateau. A compact multi-barrel pellet injector system developed by the ORNL (Oak Ridge National Laboratory) has been installed in the TJ-II stellarator. It is a four-barrel

system destined for use both as an active plasma diagnostic and as a plasma fueling source. In order to achieve both objectives it will be sufficiently flexible to allow frozen hydrogen pellets with diameters from 0.4 to 1 mm to be formed and accelerated to velocities between 100 and 1000 m s⁻¹ [8-12]. The used LP has been previously reported [2] and its luminescent screen was made of TG-Green (decay time of 500 ns), with a range of measurement between 1-30 keV.

EXPERIMENTAL RESULTS AND DISCUSSION. We have shown in previous works how energy distribution function of escaping suprathermal ions, $f(W)$, behaves in TJ-II plasmas produced solely by ECRH [2,13]. Here, we study how the population of fast ions and their distribution function behave in two types of NBI plasmas, one providing the target plasma by ECRH and the second initiating the plasma by the NBI with the help of a small loop voltage provided by the field rise.

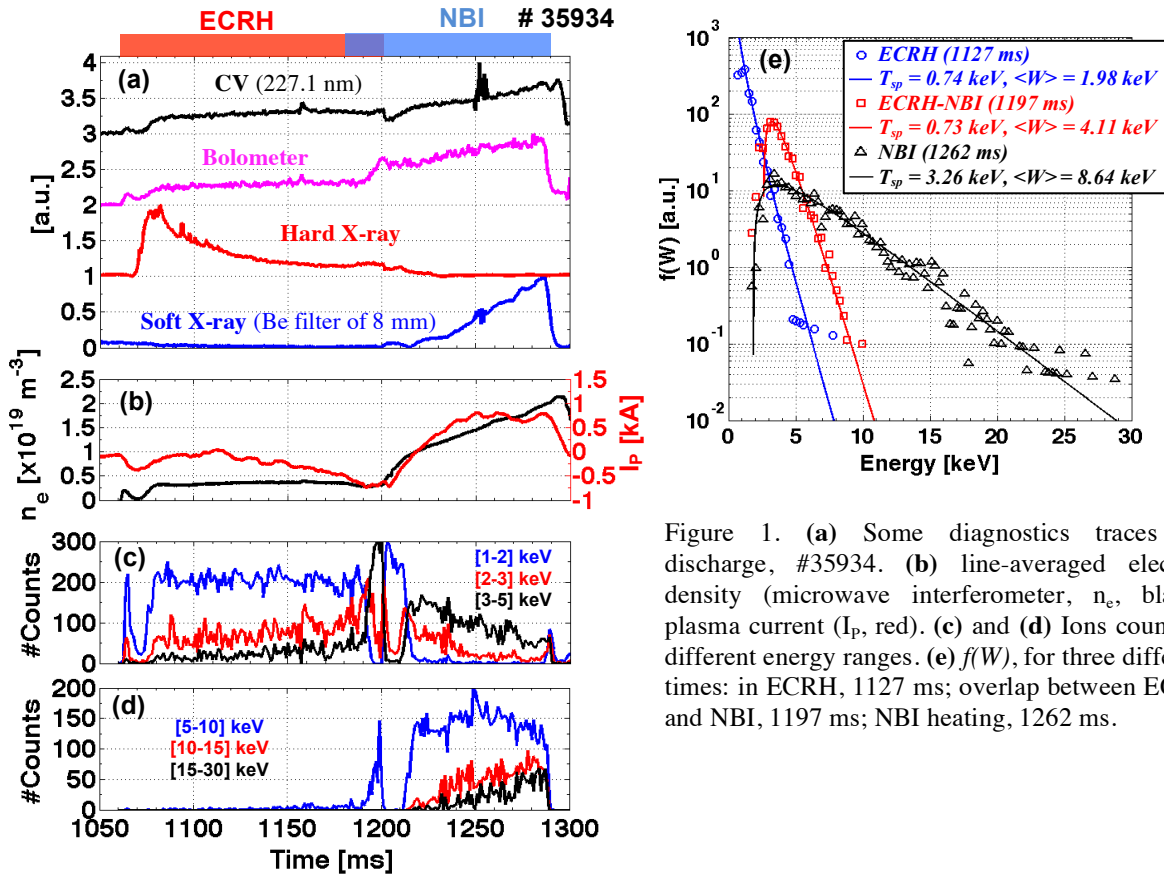


Figure 1. (a) Some diagnostics traces for discharge, #35934. (b) line-averaged electron density (microwave interferometer, n_e , black), plasma current (I_p , red). (c) and (d) Ions counts in different energy ranges. (e) $f(W)$, for three different times: in ECRH, 1127 ms; overlap between ECRH and NBI, 1197 ms; NBI heating, 1262 ms.

Figures 1(a) and 1(b) show some diagnostics traces for a discharge with ECRH (1060-1200 ms) and NBI heating (1180-1290 ms). There is an overlap between ECRH and NBI (1180-1200 ms). In figures 1(c) and 1(d), we show the ion counts per millisecond (ms) in different energy windows. It is noted that ions with energy less than 2 keV dominate in ECR heating. In the overlap, with ECRH and NBI heating, the number of ion counts with low (high) energy

decreases (increases) in a few milliseconds (< 10 ms). During the NBI heating, the dominant ion counts are those with high energies > 5 keV, that is reflected in the $f(W)$, as shown in figure 1(e), where the $f(W)$ for three phases of the discharge is exposed.

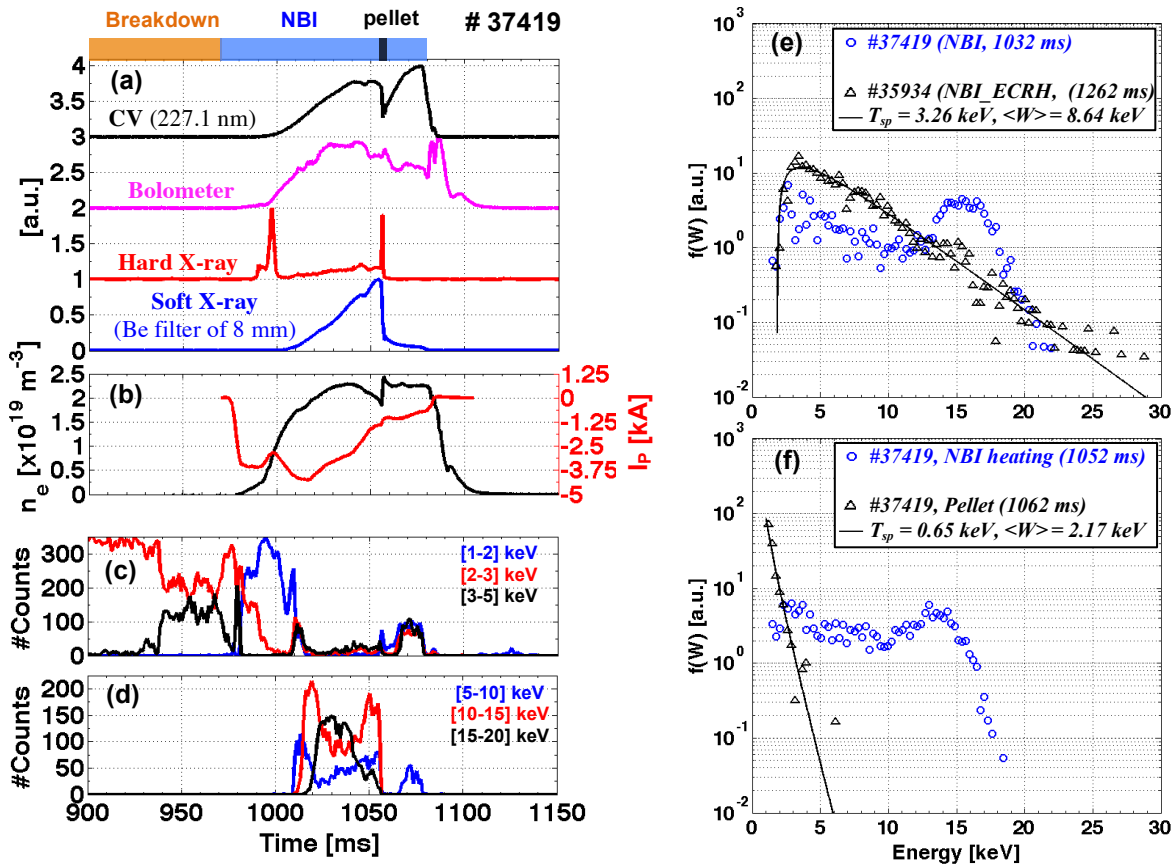


Figure 2. (a) Some diagnostics traces for discharge, #37419. (b) line-averaged electron density (n_e , black), plasma current (I_p , red). (c) and (d) shows ions counts in different energy ranges. (e) General shapes of $f(W)$ for discharges in NBI heating, (blue, #37419) solely initiated by NBI and (black, #35934) started by ECRH. (f) $f(W)$ for discharge solely with NBI heating. (blue, 1052 ms) $f(W)$ before the pellet injection, (black, 1062 ms) $f(W)$ during pellet injection.

During ECRH and overlap phase, we see that the $f(W)$ are practically the same, including the value of the temperature of suprathermal ions, T_{sp} . But expected value of energy, $\langle W \rangle$, moves to higher energies. On the other hand, in the NBI heating phase, it is observed high energy tails in $f(W)$. The second experiment (solely NBI heating [5]), needs a breakdown produced by an electric field, see figure 2. This is the best example to show whether it is possible for a loop voltage to generate suprathermal ions. During the ramp-up of current in coils CC and HX, the LP detects fast ions with high energies 2-5 keV (figure 2(c)). The NBI heating begins at 970 ms, then there is a significant change in the energy of ions until 1010 ms, with only ions < 2 keV, what coincides with the rise of the I_p (figure 2(b)), when plasma is warming. During the electron density plateau (> 1010 ms), the ions energy increases up to values higher than 15 keV, see figure 2(d). Now we investigate the effect of the pellet injection (frozen

hydrogen of diameter 1mm is introduced at 1057 ms) on suprathermal ions in the discharge #37419. Figure 2(a) shows how some plasma monitors react at the pellet injection, hard X-ray exhibit a peak in contrast with CV and soft X-rays that both decrease in response to pellet injection as it was to be expected from a sudden cooling of the plasma. Figure 2(b) shows n_e and I_p signals, both exhibit changes in response to pellet injection. Figure 2(d) shows how the suprathermal ion counts are affected, they fell drastically, but after a time ~ 10 ms the LP signal rise again with ions energy < 10 keV, see figure 2(c) and 2(d).

All these changes along discharges affect $f(W)$. In figure 2(e), the first point to note is the shape of the distributions from a discharge with ECRH and NBI heating (#35934, 1262 ms) and another with solely NBI heating (#37419, 1032ms). In the first case, the influence of NBI heating on suprathermal ions gives them more energy and make the tail of the distribution wider. But in the second case (solely NBI heating), it seems that NBI favours that the number of ions increases in a specific range of energies (12-18 keV), and it does not generate tails with higher energies (see figure 2(e)). Finally, the pellet injection causes a thermalization of suprathermal ions distribution (ions < 7 keV, see figure 2(f)). The temperature is very similar to ECRH case (figure 1(e), 1127 ms), where $f(W)$ is thermalized. However, this effect only lasts ~ 10 ms, and then the ion energy increases up to < 14 keV, but ions at higher energies (> 14 keV) do not reappear.

ACKNOWLEDGEMENTS. This work was partially funded by the Spanish “Ministerio de Economía y Competitividad” under Grant No. ENE2014-56517-R. One of the authors (M. M.) would like to thank CONACYT (Mexico) for his scholarship. This project has received funding from the European Union’s Horizon 2020 research and innovation programme under grant agreement number 633053. The views and opinions expressed herein do not necessarily reflect those of the European Commission.

REFERENCES

- [1] Zurro B, Baciero A, Tribaldos V et al., *Nucl. Fusion* **53**, 083017 (2013).
- [2] Martínez M, Zurro B, Baciero A, Jiménez-Rey D and Tribaldos V, IAEA 25th Fusion Energy Conference (FEC 2014).
- [3] Jiménez-Rey D, Zurro B et al, *Rev. Sci. Instrum.* **79**, 093511 (2008).
- [4] Zurro B, Baciero A et al., *Rev. Sci. Instrum.* **83**, 10, 10D306 (2012).
- [5] Tabarés F L, et al. Stellarator News, published by Oak Ridge National Laboratory, Issue 144, August 2014.
- [6] Alejaldre C, et al., *Fusion Technol.* **17**, 131 (1990).
- [7] Papular R, *Nucl. Fusion* **16**, 37 (1976).
- [8] McCarthy K J et al., Proc. 21st IEEE/NPSS Symposium on Fusion Engineering 2005.
- [9] McCarthy K J et al., *Rev. Sci. Instrum.* **79**, 10F321 (2008).
- [10] Combs S K et al., Proceedings 2011 IEEE/NPSS 24th Symposium on Fusion Engineering, Chicago (2011).
- [11] Combs S K, *Rev. Sci. Instrum.* **64**, 1679 (1993).
- [12] Milora S L, Houlberg W A, Lengyel L L, and Mertens V, *Nucl. Fusion* **35**, 657 (1995).
- [13] Martínez M, Zurro B, Baciero A, Jiménez-Rey D and Tribaldos V, Proc. 41st EPS conference (2014).